Complex Formation of Alkyl-*N*-iminodiacetic Acids and Hard Metal Ions in Aqueous Solution and Solid State

Cecilia Lindblad[1] · Anders Cassel[2,3] · Ingmar Persson[1]

Abstract

The calcium(II), iron(III) and chromium(III) alkyl-*N*-iminodiacetate systems have been studied in aqueous solution with respect to stability, acid–base properties and structure. The calcium(II) ion forms only one weak complex with methyl-*N*-iminodiacetic acid in water, $K_1 = 12.9$ (2) $mol^{-1} \cdot dm^3$, while iron(III) and chromium(III) form very stable complexes with alkyl-*N*-iminodiacetic acids. The calcium(II)–methyl-*N*-iminodiacetate complex is octahedral in the solid state with most probably water in the remaining positions giving a mean Ca–O bond distance of ca. 2.36 Å. The iron(III) alkyl-*N*-iminodiacetate complexes have low solubility due to a strong tendency to form polymeric structures. Depending on pH in the solution at their preparation, the degree of hydrolysis in the resulting compound(s) may differ. In the solid state, the polymeric iron(III) alkyl-*N*-iminodiacetate compounds seem to have the mean composition $Fe_2O(C_x\text{-IDA})_5$; the mean Fe–O bond distances to the oxo group and the alkyl-*N*-iminodiacetate ligands are 1.92 and 2.02 Å, respectively. In these complexes the nitrogen atoms are bound at much longer bond distances, 0.1–0.2 Å, than the carboxylate oxygens. This distribution with short strong Fe–O bonds and much longer and weaker Fe–N bonds is also found in most other structurally characterized iron(III) carboxylated amine/polyamine complexes. The chromium(III) alkyl-*N*-iminodiacetate complexes are octahedral in both solution and solid state, and the low solubility of the solid compounds indicates a polymeric structure with the ligands bridging chromium(III) ions. Also, chromium(III) binds oxygen atoms in carboxylated amines at significantly shorter distance than the nitrogen stoms. The chromium(III) alkyl-*N*-imino-diacetate complexes display such slow kinetics at titration with strong base that the back-titration with strong acid shows completely different acid–base properties, thus the acid–base reactions are irreversible.

✉ Ingmar Persson
Ingmar.Persson@slu.se

Extended author information available on the last page of the article

1 Introduction

Interest is growing for chelating surfactants in technical applications such as separation of metal ions and complexes from, e.g., industrial wastewater and polluted soils. In order to develop specificity of the chelating surfactants, more detailed knowledge of their physico-chemical and structural behavior is required. Many chelating surfactants on the market are technical products containing several similar compounds, but this means that detailed physico-chemical studies cannot be performed accurately. The most common type of chelating surfactants, alkyl-polyamine carboxylates, so called APACs, consists of a hydrocarbon chain and a hydrophilic chelating part [1]. In this project we have chosen to study the simplest chelating surfactants of this kind, alkyl-*N*-iminodiacetic acids (IUPAC name alkyl-*N*-iminodiethanoic acids), as they can be prepared with high purity.

The acidic constants of the iminodiacetic and alkyl-*N*-iminodiacetic acids show that they are present as zwitter ions in aqueous solution as the imino nitrogen is a much stronger base than the carboxylate groups, see supplementary Table S1. The acidic constants show also that the acetic acid groups are significantly stronger acids in iminodiacetic and alkyl-*N*-iminodiacetic acid than in acetic acid itself, while for the imino group the acid–base properties are similar to those of the ammonium and alkyl ammonium ions [2].

The alkyl-*N*-iminodiacetates are reported to form moderately stable complexes with calcium(II) and very stable complexes with iron(III) and chromium(III), Tables S2–S4. It is important to verify the composition of the complexes present in the systems under study, and thereby the definition of the stability constants. In the determination of the stability constants of the metal-alkyl-*N*-iminodiacetic acid systems it has been taken for granted that the nitrogen atom is bound to the metal ion and thereby deprotonated, Tables S2–S4. Whether this is correct or not will have large implications on the description of these systems. It is therefore important to determine the structure at the molecular level of the complexes.

The metal ions investigated in this study, calcium(II), chromium(III) and iron(III), are typically hard metal ions and the chelating surfactants used are methyl-, *n*-hexyl-, *n*-dodecyl- and *n*-octadecyl-*N*-iminodiacetic acids. The stability constants of the calcium complexes were determined potentiometrically with a calcium ion selective electrode. Crystal structures of the limited number of calcium(II), chromium(III) and iron(III) iminodiacetate and alkyl-*N*-iminodiacetate complexes are summarized in Tables S5–S7.

Two crystal structures containing calcium iminodiacetate complexes have been reported in the literature, catena-(bis(μ$_3$-hydrogeniminodiacetate)calcium, (Ca(HN(CH$_2$COO)$_2$)$_n$ [3], and catena-(μ$_4$-*N*-2-hydroxyethyliminodiacetate-O,O′,O″) calcium trihydrate, (CaC$_6$H$_9$NO$_5$)$_n$·3nH$_2$O [4], Table S5. In the first compound calcium binds only to oxygen atoms in an octahedral fashion at a mean Ca–O bond distance of 2.320 Å [3]. In the latter compound only one iminodiacetate ligand is bound to calcium. In this compound calcium is seven-coordinated by six oxygens, mean 2.414 Å, and one nitrogen atom, 2.591 Å [4]. In both compounds the imino nitrogen is protonated. These crystal structures are polymeric where the same iminodiacetate ion binds to calcium in chains or networks. This situation is not expected to persist in aqueous solution where the reported stability constants show the presence of monomeric complexes, Table S2.

Five crystal structures containing iminodiacetato- or alkyl-*N*-iminodiacetaferrate(III) complexes have been reported, Fe(R−N)(CH$_2$COO)$_2$)$_2^-$, R=H [5–7], R=CH$_3$ [8] and R=CH$_2$COO$^-$ [9], Table S6. In three of these structures [6–8], the mean Fe–O and Fe–N bond distances are 1.977 and 2.155 Å, respectively, showing a significantly shorter and

stronger binding to oxygen donor atoms than to nitrogen atoms. A similar binding pattern is observed in the iminodiacetato- and alkyl-*N*-iminodiacetatochromate(III) complexes with mean Cr–O and Cr–N bond distances of 1.956 and 2.087 Å, respectively, Table S7. This is expected as the hard electron-pair acceptors iron(III) and chromium(III) prefer binding to the harder oxygen than to the softer nitrogen. Thirteen crystal structures containing chromium(III) iminodiacetate or alkyl-*N*-iminodiacetate complexes have been reported, $Cr(R-N)(CH_2COO)_2^-$, R = H [10–12], R = CH_3 [13–15], R = CH(CH_3)_2 [16], R = C(CH_3)_3 [17], R = CH_2CH_2OH [18], R = CHCONH_2 [19, 20] and R = CH_2COOH [21]. In these complexes chromium(III) binds strongly to four oxygen atoms from the carboxylate groups, mean of 1.96 Å, and to two imine nitrogens at significantly longer bond distance, mean 2.09 Å, see Table S7 for details.

In the present study the structures of calcium, chromium(III) and iron(III) complexes with methyl, *n*-hexyl-, *n*-dodecyl- and *n*-octadecyl-*N*-iminodiacetate in the solid state have been performed by EXAFS as it has not been possible to get single crystals of sufficient size and quality for crystallographic investigations. Stability constants of these systems in aqueous solution have been determined using calcium, chromium(III) and iron(III) ion selective electrodes.

The aim of this study is to get increased knowledge about complex formation, structures and physico-chemical properties of calcium, iron(III) and chromium(III) complexes with surface active ligands such as alkyl-*N*-iminodiacetates with varying alkyl chain length. This will form the basis for the development of suitable surface active compounds to bind and separate metal ions and compounds for industrial and technical applications.

2 Experimental Section

2.1 Chemicals

Methyl-N-iminodiacetic acid, $CH_3N(CH_2COOH)_2$ (Aldrich, 99%), perchloric acid 70–72% (Merck, p.a.), sodium hydroxide solution (Merck, Titrisol), calcium carbonate (Merck, 99.0%), sodium perchlorate monohydrate, $NaClO_4 \cdot H_2O$ (Merck, p.a., ≤99.0%), ferric perchlorate hexahydrate, $[Fe(H_2O)_6](ClO_4)_3$ (GFS Chemicals, ≤99.9%), chromium(III) perchlorate hexahydrate, $[Cr(H_2O)_6](ClO_4)_3$ (GFS Chemicals, ≤99.9%), calcium perchlorate tetrahydrate, $Ca(ClO_4)_2 \cdot 4H_2O$ (Aldrich, 99%), boron nitride, BN (Aldrich, ≤99.5%), potassium chloride, KCl (Merck, p.a., ≤99.95%) were used as purchased. n-Hexyl-, n-dodecyl- and n-octadecyl-N-iminodiacetic acid, $RN(CH_2COOH)_2$, R = *n*-C_6H_13, *n*-C_12H_25 and *n*-C_18H_37, respectively, were prepared as described elsewhere [22], and were used without further treatment. The water used was deionized and filtered by a Milli-Q® filter system giving water with 18.2 MΩ·cm resistance.

2.2 Sample Preparation

Aqueous stock solutions of 20.2 mmol·dm^{-3} Ca(ClO_4)_2, pH adjusted to 1.91 with perchloric acid, and 99.9 mmol·dm^{-3} methyl-*N*-iminodiacetic acid, pH 2.08, were prepared for the potentiometric measurements. The ionic strength was adjusted with a 2 mol·dm^{-3} KCl solution, 1 mL per 25 mL titrand. For titrations at neutral pH, the calcium and methyl-*N*-iminodiacetic acid solutions were pH adjusted by a NaOH solution. Aqueous solution containing 19.52 mmol·dm^{-3} calcium at pH 7.53 and 91.0 mmol·dm^{-3} methyl-*N*-iminodiacetate

solution at pH 7.04 were used in the titrations. For titration with large excess of ligand a 1.95 mmol·dm^{-3} Ca(ClO$_4$)$_2$ solution, pH 7.53, was used.

2.2.1 Acid/Base Titrations of Chromium(III)–Methyl-*N*-iminodiacetic Acid (1:2)

A stock solution of 0.015 mol·dm^{-3} Cr(ClO$_4$)$_3$ was prepared, containing 0.015 mol·dm^{-3} HClO$_4$ to prevent from hydrolysis of chromium(III), pH 1.764; the color of this solution is indigo. A 0.10 mol·dm^{-3} methyl-*N*-iminodiacetic acid solution at pH$_{ie}$ 1.784 was used as stock solution. The titrand solution used was 0.0114 and 0.0231 mol·dm^{-3} in respect to chromium(III) and methyl-*N*-iminodiacetic acid, respectively, pH 1.853. The color of the solution was indigo. 0.0997 mol·dm^{-3} NaOH and 0.1000 mol·dm^{-3} HClO$_4$ were used as titrators.

For the acid/base titrations of chromium(III)/*n*-hexyl-*N*-iminodiacetic acid (1:3), 4.5×10^{-4} mol Cr(ClO$_4$)$_3$ was dissolved in 0.45 mL 1.0 mol·dm^{-3} HClO$_4$, 2.25 mL (600 mmol·dm^{-3} hexyl-*N*-iminodiacetic acid, one equivalent NaOH) and 1.00 cm^3 water were added; the titrator was an aqueous solution of 0.0997 mol·dm^{-3} NaOH.

As the sample preparation for the EXAFS measurements, dried precipitates of calcium/hexyl-*N*-iminodiacetic acid/OH$^-$ from aqueous solutions (molar ratios 1:1:2 and 1:3:6) were ground without any addition of boron nitride. These samples became pasty and flaky upon grinding. The samples were placed in 0.5 mm Al-frames which were covered on the backside with Mylar tape and on front-side with X-ray polypropylene film (6 μm). Previously reported studies on the hydrated calcium ion in aqueous solution were used as reference [23].

The dried precipitates of iron(III)/*n*-hexyl-*N*-iminodiacetic acid/OH$^-$ from aqueous solutions with molar ratios of 1:1:0, 1:3:0, 1:1:1, 1:3:3 and 1:1:2, and iron(III)/*n*-dodecyl-*N*-iminodiacetic acid/OH$^-$ from aqueous solutions with molar ratios of 1:1:1 and 1:2:1 were ground with BN (30–40 wt%). The cells used were typically ca. 1.0 mm Ag- or Al-frames covered by Mylar tape. The precipitates were dried and ground with BN (40 wt%). The cells used were 0.5–0.9 mm Ag-frames covered by Mylar tape. For the aqueous solutions of 10 mmol·dm^{-3} iron(III)/*n*-hexyl-*N*-iminodiacetic acid/OH$^-$ (1:1:0, pH 1.63 and 1:5:0, pH 2.50), the sample cell was 10 mm Teflon spacers and X-ray polypropylene film windows held together with brass frames were used.

The dried precipitate of chromium(III)/*n*-hexyl-*N*-iminodiacetic acid/OH$^-$ from aqueous solution with the molar ratio 1:3:3 became pasty upon grinding and no BN was added. The paste was pressed into a 0.5 mm thick Ag-frame covered on back and front with Mylar tape. For the aqueous solutions of chromium(III)/*n*-hexyl-*N*-iminodiacetic acid/OH$^-$ (1:3:3, pH 2 and 58 mmol·dm^{-3} chromium(III), 1:3:≈3, pH 4.10), the same cells as in the measurements of the aqueous solutions of iron(III) but with 2–5 mm Teflon spacers instead.

2.3 Potentiometry

The acid–base titrations and occasional pH measurements were performed using an Orion Research EA 940 potentiometer with a Mettler Toledo InLab®422 pH electrode. Calibrations were performed with Orion standards at pH (4.01, 7.00 and 10.01). All measurements were performed at ambient room temperature, 295 ± 1 K, and with gentle magnetic stirring. The titrants were manually added by a digital burette (Brand Bürette Digital II) or an analogue glass burette. The calcium ion potentiometry set-up was the same as for the pH measurements but with a calcium ion selective electrode (Orion 97-29 Ionplus Calcium

Combination Electrode) calibrated by calcium perchlorate standards of (0.010, 0.0010, and 0.00010) mol·dm^{-3}. The evaluation of the β_1 stability constant was made numerically with the use of the program EMFALL [24], and the acidic constants reported elsewhere [22].

2.4 EXAFS

The EXAFS spectra were recorded at Stanford Synchrotron Radiation Lightsource, wiggler beam line 4-1, old station. A Si(111) double crystal monochromator was used. For the calcium studies the entire experimental set-up was placed in a helium filled bag to minimize air absorption and scattering. Helium was used in ion chamber I_0 and the sample compartment and nitrogen was used in ion chambers I_1 and I_2 and in the Lytle detector. For external calibration, a tin foil (Sn L_3 edge, 3929 eV) [21] was recorded before and after each sample. For the iron(III) and chromium(III) samples, nitrogen was used in all ion chambers and argon in the Lytle detector. Internal energy calibration was performed by simultaneously recording an iron or chromium foil, with the first inflection point on each edge defined as 7111.3 and 5989.0 eV, respectively [25].

The data treatment and model fitting of the EXAFS data has been carried out using the EXAFSPAK package [26], using standard procedures for pre-edge subtraction and spline removal. The resulting EXAFS functions have been curve-fitted by calculated model functions using ab initio calculated EXAFS phase and amplitude functions from FEFF7 (version 7.02) [27]. Theoretical back-scattering amplitude functions were calculated for each coordination shell of back-scattering by oxygen, nitrogen, carbon and metal atoms including multiple scattering paths. Each set of EXAFS data was optimized using paths from each coordination shell. The back-scattering in the iron complexes were modeled with both dihydroxo bridged, and linear and tilted μ-oxo bridged iron scattering paths. Redundant paths were discarded and the most prominent scattering paths were kept in order to find the structure of the complex under study.

3 Results and Discussion

3.1 The Calcium(II) Alkyl-*N*-iminodiacetic Acid Systems in Water

3.1.1 Determination of Stability Constants Using Potentiometry

The calcium solutions were clear and colorless before, during and after titrations. The variation in pH during the titrations was very small showing that no (or negligible) proton release takes place, Fig. S1. This shows that the nitrogen in the methyl-*N*-iminodiacetic acid remains protonated with complex formation. The small changes in the free calcium ion concentration during the titrations show that the complex formation is weak with only one complex formed, $\log_{10} K_1 = 12.9(2)$ mol·dm^{-3}. This low stability constant strongly indicates that the methyl-*N*-iminodiacetic acid binds as a monodentate ligand. The stability constants of the calcium(II) formate and acetate systems, $\log_{10} K_1 = 1.43$ [28, 29], and 1.24 [29], 1.12 [30, 31] and 1.2 [32], respectively, at zero ionic strength giving, after extrapolation, $\log_{10} K_1 \approx 1.0$ and 0.7 at 0.1 mol·dm^{-3} ionic strength, while the stability constants of the calcium(II) oxalate system are significantly larger, $\log_{10} K_1 = 2.54$ ($I = 0.1$ mol·dm^{-3} NaCl) [33] and 2.30 ($I = 0.1$ mol·dm^{-3} KNO$_3$) [34]. The stability constant of the calcium(II)–methyl-*N*-iminodiacetate complex measured in this study has the same

order of magnitude as for the monodentate formate and acetate ligands, while the biden-
tate oxalate ion forms significantly stronger complexes (probably bidentate in the chelate
form). This further supports the idea that the methyl-*N*-iminodiacetate binds to calcium
as a monodentate ligand in aqueous solution. The previously reported stability constants
of the calcium(II) iminodiacetate and alkyl-*N*-iminodiacetate systems are several orders of
magnitude higher than found in the present study, Table S2. If it is assumed that the nitro-
gen atom is involved in the complex formation it will cause that larger stability constants
are obtained for the same experimental pH data than they are in reality.

3.1.2 Structure Determination Using EXAFS

The Fourier transforms of the studied calcium samples (Fig. S2, the data are not cor-
rected for the phase shift) show a major peak at ca. 2.35 Å corresponding to a first shell of
approximately six-coordinated oxygen atoms [22]. At 4.7 Å there is a small and broad dis-
tribution related to the multiple scattering within the octahedral CaO_6 core. A small peak
at ca. 3.0 Å corresponds to a second shell of carbon atoms with a Ca–O–C 3-leg scatter-
ing contribution at ca. 3.4 Å. The Ca–O bond distances were refined to 2.35 (1) and 2.37
(1) Å in two calcium samples, Table 1, and the three- and four-legged multiple scattering
paths at double Ca–O bond distance, $d(Ca–O_{MS}) = 4.78(4)$ Å. The second shell Ca⋯C dis-
tance was refined to 3.01(1) Å and the 3-leg Ca–O–C multiple scattering path to 3.34(2)
Å in the sample with excess of ligand; the Ca–O–C bond angle is close to tetrahedral. In
the sample with low ligand concentration a Ca⋯C distance of 3.21 Å was found, reflect-
ing a mean value of the single and multiple scattering paths. Neither nitrogen nor calcium
ions were found in the inner coordination shell. The calcium EXAFS raw data show some
small peculiar shoulders at low *k*-values, ca. 2.5 and 4.2 Å^{-1}, Fig. 1, which might be multi-
ple electron excitations [35, 36], which were allowed to remain in the refined data as they
did not influence the refinements. The distances and other parameters are summarized in
Table 1 and the fitting of the EXAFS data are given in Fig. 1.

The Ca-O bond distance and the multiple scattering with the CaO_6 core show that the
calcium(II) ion has a basic octahedral structure in solid state, when binding one or several
alkyl-*N*-iminodiacetate ligands. Thus, the complex formation causes a reduction in coor-
dination number from eight to six upon complex formation. It is not possible from the
present data to determine whether the alkyl-*N*-iminodiacetate ligands are monodentately
bound or bridging by two calcium ions in the solid state.

Table 1 Mean bond distances, d/Å, Debye–Waller factors, σ^2/Å^2, number of distances, N, and the shift in the threshold energy, ΔE_o/eV, of calcium(II)-*n*-hexyl-*N*-iminodiacetate complexes in solid state at room temperature

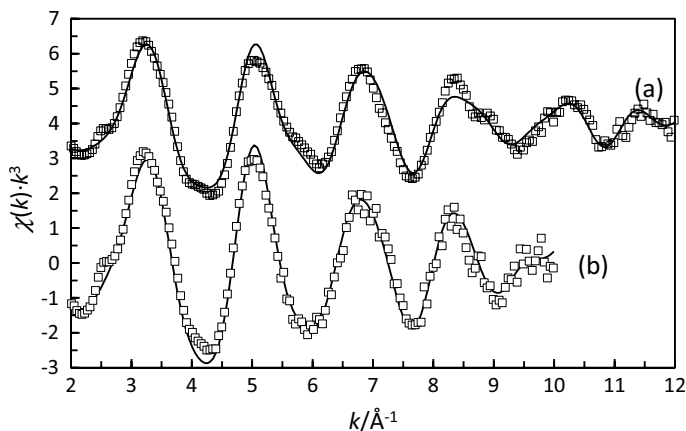| Interaction	N	d	σ^2	ΔE_o[a]	S_o^2
Ca^{2+}/*n*-hexyl-*N*-iminodiacetic acid/OH$^-$(1:1:2)					
Ca–O	6	2.351 (7)	0.0093 (9)	−13.9 (5)	0.55 (2)
Ca–O–O	24	4.09 (8)	0.007 (2)		
MS (CaO$_6$)	3×6	4.71 (3)	0.005 (2)		
Ca⋯C/Ca–O–C	4	3.22 (2)	0.009 (2)		
Ca^{2+}/*n*-hexyl-*N*-iminodiacetic acid/OH$^-$(1:3:6)					
Ca–O	6	2.379 (9)	0.0102 (12)	−12.4 (5)	0.82 (4)
Ca–O–O	24	4.13 (10)	0.004 (3)		
MS (CaO$_6$)	3×6	4.77 (3)	0.005 (2)		

Fig. 1 Fit of EXAFS data of solid calcium(II) *n*-hexyl-*N*-iminodiacetate complexes precipitated from aqueous solution with the composition (a) calcium(II)/*n*-hexyl-*N*-iminodiacetic acid/OH⁻(1:1:2) and (b) calcium(II)/*n*-hexyl-*N*-iminodiacetic acid/OH⁻(1:3:6). The experimental data points are shown as open squares, and lines were calculated with the models using the parameters given in Table 1 as solid lines

3.2 The Iron(III) Alkyl-*N*-iminodiacetic Acid Systems in Water

3.2.1 Precipitation Reactions

100 mmol·dm^{-3} iron(III) perchlorate, pH 1.73, and 100 mmol·dm^{-3} *n*-hexyl-*N*-iminodiacetic acid, pH 1.96 (isoelectric pH), were mixed in molar ratios 1:1, 1:2 and 1:3. All samples resulted in pale rust-red precipitations and the pH was measured in the pale yellow supernatant. The proton release seems to be constant as a function of iron(III) concentration. The proton release emanates most probably from a continuing hydrolysis of the partially hydrolyzed iron(III) ions and complexes. When mixing the same solutions at higher pH, a similar pale rust-red precipitate was formed when the molar ratio was 1:1, but when the molar ratio was 1:3 a dark brownish-red and compact precipitate was formed.

For 100 mmol·dm^{-3} iron(III) solutions the 1:1 sample results in a pale yellow supernatant and a pale rust-red precipitate; 1:3 results in a colorless supernatant and a pale rust-red precipitate which turns into a lemon yellow and water swollen precipitate after one week of aging. The latter precipitate is stable over months.

These samples were diluted ten times with water and heavily ultra-sonicated. The samples were partly dissolved into a lemon yellow supernatant with only a small amount of precipitate remaining. After months of aging the precipitate was completely dissolved and the solution was colorless.

For a 10 mmol·dm^{-3} iron(III) solution the 1:1 sample results in a lemon yellow solution, and the 1:2 and 1:5 samples result in a lemon yellow supernatant and a small amount of a pale rust-red precipitate, which dissolve into a colorless solution after months of aging. The lemon yellow precipitate from the 1:3 (100 mmol·dm^{-3} iron(III) solution) sample was dried and dissolved in chloroform (1.4 wt‰) resulting in an extremely viscous and completely clear yellow and fully transparent solution. The complex soluble in chloroform is most probably neutral, and with the alkyl groups strongly solvated as seen in the resulting viscous solution.

The light yellow precipitates and solutions seem to contain neutral chelate complexes of iron(III) alkyl-*N*-iminodiacetate, e.g. as seen by their reasonable solubility in water and chloroform. The pale rust-red compounds display low solubility also in water, independent of the iron(III)–alkyl-*N*-iminodiacetate proportions, which indicates that these compounds are polymeric in nature.

3.2.2 EXAFS Analysis on Iron(III)/Alkyl-*N*-iminodiacetate Complexes in Solid State and Solution

The EXAFS data of the solid iron(III) alkyl-*N*-iminodicate compounds precipitated at different iron(III)/alkyl-*N*-iminodicate/hydroxide ion ratios and two aqueous solutions are shown in Fig. 2. The EXAFS spectra and the Fourier transforms (FTs) of solid compounds precipitated at low iron(III)/alkyl-*N*-iminodiacetate ratios with none or one equivalent of sodium hydroxide (FeC$_{12}$_1:1:1, FeC$_{12}$_1:2:1, FeC$_6$_1:1:0 and FeC$_6$_1:1:1) are almost identical, Figs. 2 and 3. The EXAFS and FTs of the solids precipitated with 2 or 3 equivalents of sodium hydroxide (FeC$_6$_1:1:2 and FeC$_6$_1:3:3) are slightly different with a broader maximum at $k = 8.5$ Å^{-1}, instead of the double maximum in the first group of EXAFS spectra, while the FTs are similar to the other solids, Fig. 2. The compound precipitated from an aqueous solution an iron(III)/*n*-hexyl-*N*-iminodiaceatate ratio of 1:3 without any addition of sodium hydroxide, (FeC$_6$_1:3:0) has a different shape around $k = 8.5$ Å^{-1}, and the peak in the FT at ca. 3 Å (without phase correction) is at longer distance, Figs. 2 and 3. The latter compound is the one formed at the lowest pH value, caused by proton release resulting from complex formation. The Fourier transforms of the studied iron(III) samples show a strong peak at ca. 3 Å (without phase correction) in the solid samples, assigned to a Fe···Fe distance. The two aqueous solutions with iron(III)/*n*-hexyl-*N*-iminodiaceatate ratios of 1:1 and 1:3 with pH 1.67 and 2.5, respectively, are very similar, even though there was a high noise level due to low concentrations. The structure around the iron(III) ion in the aqueous solutions is similar to the ones observed in the solids, Figs. 2 and 3.

The major peak in the Fourier transforms (FTs) observed in all samples correspond to a first shell of oxygen atoms at ca. 1.5 Å (without phase shift correction), Fig. 3, and refined to ca. 2.0 Å. It can also be seen that this peak is somewhat asymmetric towards shorter distances in the solids and the aqueous solutions, Fig. 3. The asymmetry of this peak indicates an additional shorter Fe–O bond distance which together with the observed Fe···Fe distance strongly indicates the presence of an oxo or hydroxo bridge between the iron(III) ions. The broad peak at 3.5 Å, refined to ca. 4.0 Å corresponds to multiple scattering within the octahedral FeO$_6$ core (Fig. 4).

Refinements of the EXAFS data of the solid samples give a good fit with a dimeric model with a hydroxo/oxo group bridging two iron(III) ions, d(Fe–O) = 1.92(1) Å, and the iron(III) ions bind four oxygen atoms completing an octahedral configuration with a mean Fe–O bond distance of 2.00–2.02 Å, and a much longer Fe–N bond at ca. 2.20 Å, Table 2. The related two bond distances from multiple scattering paths within the FeO/N$_6$ core are observed in the expected range, Table 2. A second shell of carbon atoms is localized at d(Fe···C) = 2.95–3.00 Å, and the corresponding 3-leg Fe–O–C scattering path is found at d(Fe–O–C) = 3.15–3.20 Å, Table 2, giving a Fe–O–C bond angle of ca. 126°, typical for carboxylate groups binding to a hard metal ion as iron(III). The strong peak in the FTs at ca. 3.0 Å (without phase correction) has been assigned to an Fe···Fe distance, which was confirmed by a back-Fourier transformation showing a maximum in the EXAFS function
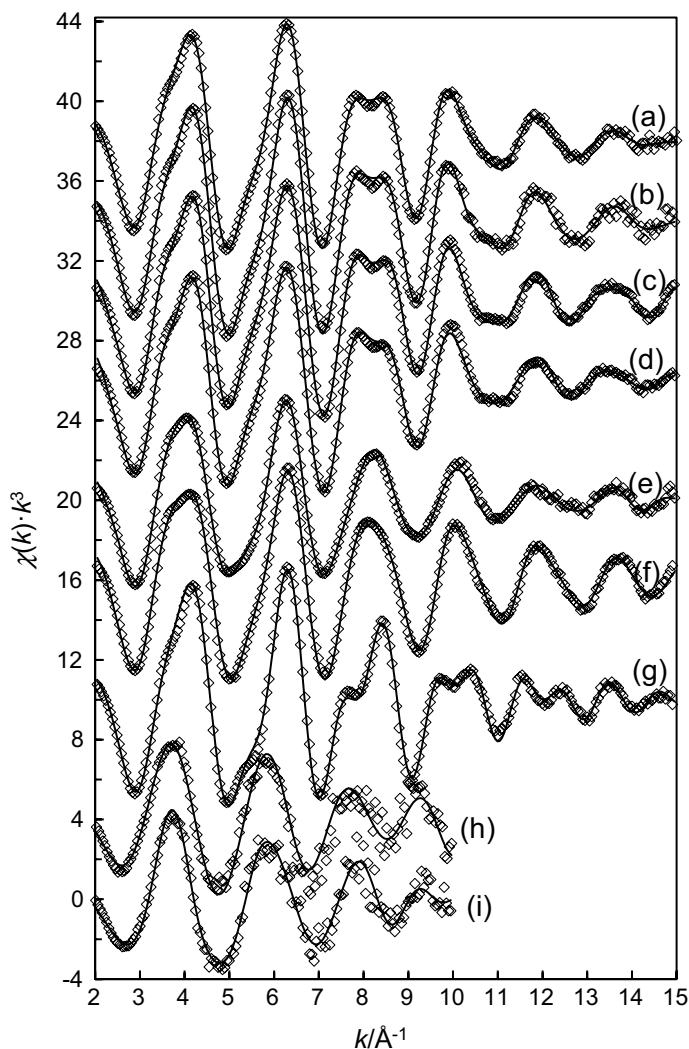
Fig. 2 Fit of EXAFS data of solid iron(III) alkyl-*N*-iminodiacetate complexes precipitated from aqueous solutions with the composition (a) iron(III)/*n*-dodecyl-*N*-iminodiacetic acid/OH⁻ (1:1:1), (b) iron(III)/*n*-dodecyl-*N*-iminodiacetic acid/OH⁻ (1:2:1), (c) iron(III)/*n*-hexyl-*N*-iminodiacetic acid/OH⁻ (1:1:0), (d) iron(III)/*n*-hexyl-*N*-iminodiacetic acid/OH⁻ (1:3:0), (e) iron(III)/*n*-hexyl-*N*-iminodiacetic acid/OH⁻ (1:1:1), (f) iron(III)/*n*-hexyl-*N*-iminodiacetic acid/OH⁻ (1:2:1), (g) iron(III)/*n*-hexyl-*N*-iminodiacetic acid/OH⁻ (1:3:0), and aqueous solutions of 10 mmol·dm⁻³ iron(III) *n*-hexyl-*N*-iminodiacetate complexes with the ratio (h) 1:1 and (i) 1:3. The diamonds are the experimental points and the solid lines were calculated with the models using the parameters given in Table 2

at 7 $Å^{-1}$ (light back-scatterer atoms as oxygen having a maximum at 4–5 $Å^{-1}$). For these solid samples the mean $d(Fe \cdots Fe)$ was determined to be ca. 3.36 Å from single scattering and the corresponding multiple scattering path was found at $d(Fe \cdots Fe_{MS}) \approx 3.6$ Å. The sample $FeC_6\_1{:}3{:}0$ has a different EXAFS spectrum in comparison to the other solids, and the FT shows that the Fe···Fe distance is longer in this sample, Fig. 3, refined to 3.43(1) Å,

Fig. 3 Fit of Fourier transforms of solid iron(III) alkyl-*N*-iminodiacetate complexes precipitated from aqueous solutions with the composition (a) iron(III)/*n*-dodecyl-*N*-iminodiacetic acid/OH⁻(1:1:1), (b) iron(III)/*n*-dodecyl-*N*-iminodiacetic acid/OH⁻(1:2:1), (c) iron(III)/*n*-hexyl-*N*-iminodiacetic acid/OH⁻(1:1:0), (d) iron(III)/*n*-hexyl-*N*-iminodiacetic acid/OH⁻(1:3:0), (e) iron(III)/*n*-hexyl-*N*-iminodiacetic acid/OH⁻(1:1:1), (f) iron(III)/*n*-hexyl-*N*-iminodiacetic acid/OH⁻(1:2:1), (g) iron(III)/*n*-hexyl-*N*-iminodiacetic acid/OH⁻(1:3:0), and aqueous solutions of 10 mmol.dm⁻³ iron(III) *n*-hexyl-*N*-iminodi-acetate complexes with the ratio (h) 1:1 and (i) 1:3. The diamonds are the experimental points and the solid lines the models using the parameters given in Table 2
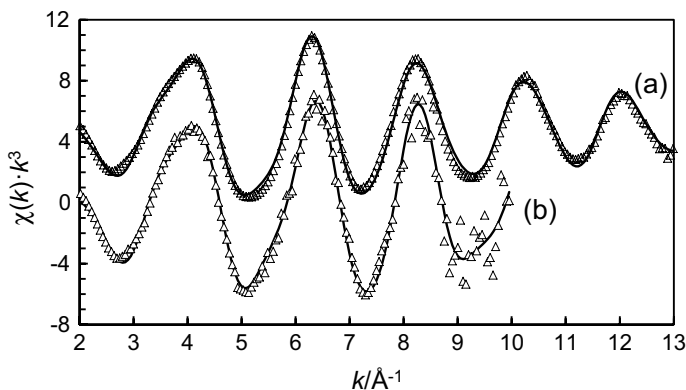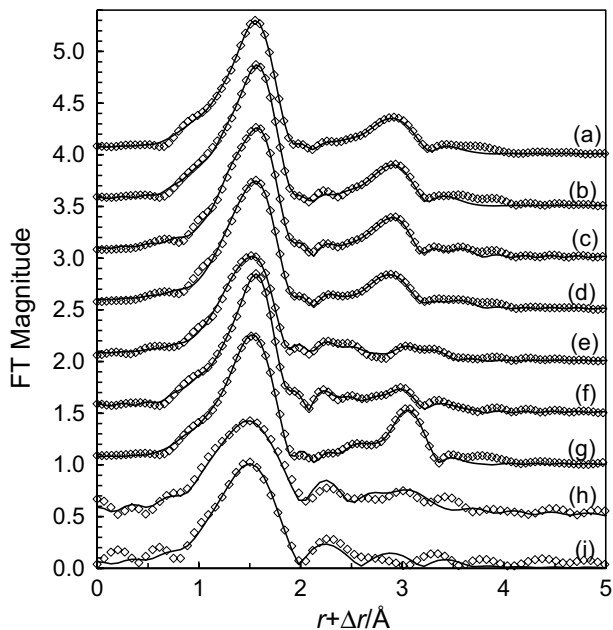

Fig. 4 Fit of EXAFS data of (a) a solid chromium(III)–*n*-hexyl-*N*-iminodiacetate complex precipitated from an aqueous solution with the composition chromium(III)/*n*-hexyl-*N*-iminodiacetic acid/OH⁻ (1:3:3), and (b) an aqueous solution of this compound at 58 mmol·dm⁻³. The solid lines with dots are the experimental points and the solid thicker lines were calculated with the model using the parameters given in Table 3

Table 2. Furthermore, it was not possible to refine any Fe–N bond distance, strongly indicating that the nitrogen atom is protonated and thereby not binding to iron, and the short Fe–O bond distance is slightly shorter than in the other solid samples.

In order to determine the kind of oxo/hydroxo bridge between the iron sites, the Fe–O and Fe···Fe distances in the solid state structures with Fe–O–Fe, Fe–OH–Fe, Fe(OH)$_2$Fe and Fe(OH)(RCOO)Fe bridges has been surveyed in the Cambridge Structure Database [37]. The Fe–O bond distance in compounds with a single oxo bridge (Fe–O–Fe) have

Table 2 Mean bond distances, d/Å, number of distances, N, and Debye–Waller coefficients, σ^2/Å^2, threshold energy, E_o, amplitude reduction factor, S_o^2, and the goodness of fit as defined in Ref. [9] from EXAFS studies of solids precipitated from aqueous solutions different iron(III)/alkyl-N-iminodiacetate/hydroxide ratios at ambient room temperature

Interaction	N	d	σ^2	E_o [a]	S_o^2	F
Solid FeC$_{12}$_1:1:1						
Fe–O	1	1.924 (3)	0.0024 (3)	–6.7 (2)	1.01 (2)	7.70
Fe–O	4	2.025 (2)	0.0049 (2)			
MS (FeO$_4$)	3 × 4	4.050	0.0063 (9)			
Fe–N	1	2.36 (1)	0.020 (3)			
Fe⋯C	4	2.973 (4)	0.0083 (5)			
Fe–O–C	8	3.162 (6)	0.0106 (6)			
Fe⋯Fe	1	3.360 (3)	0.0075 (3)			
Solid FeC$_{12}$_1:2:1						
Fe–O	1	1.933 (2)	0.0047 (2)	–6.7 (2)	0.96 (2)	10.07
Fe–O	4	2.017 (3)	0.0059 (3)			
MS (FeO$_4$)	3 × 4	4.033	0.0063 (9)			
Fe–N	1	2.36 (1)	0.013 (2)			
Fe⋯C	4	2.968 (5)	0.0099 (7)			
Fe–O-C	8	3.148 (7)	0.0114 (7)			
Fe⋯Fe	1	3.367 (4)	0.0064 (4)			
Solid FeC$_6$_1:1:0						
Fe–O	1	1.928 (3)	0.0034 (3)	–6.7 (2)	0.95 (2)	9.05
Fe–O	4	2.015 (2)	0.0053 (3)			
MS (FeO$_4$)	3 × 4	4.030	0.0073 (9)			
Fe–N	1	2.35 (1)	0.018 (2)			
Fe⋯C	4	2.964 (4)	0.0087 (5)			
Fe–O–C	8	3.157 (6)	0.0111 (7)			
Fe⋯Fe	1	3.359 (3)	0.0072 (3)			
Solid FeC$_6$_1:1:1						
Fe–O	1	1.918 (3)	0.0039 (3)	–6.7 (2)	0.89 (2)	7.70
Fe–O	4	2.012 (2)	0.0049 (2)			
MS (FeO$_4$)	3 × 4	4.024	0.0063 (9)			
Fe–N	1	2.36 (1)	0.020 (3)			
Fe⋯C	4	2.973 (4)	0.0083 (5)			
Fe–O–C	8	3.162 (6)	0.0106 (6)			
Fe⋯Fe	1	3.357 (3)	0.0008 (4)			
Solid FeC$_6$_1:1:2						
Fe–O	1	1.924 (3)	0.0024 (3)	–6.7 (2)	1.01 (2)	7.70
Fe–O	4	2.025 (2)	0.0049 (2)			
MS (FeO$_4$)	3 × 4	4.050	0.0063 (9)			
Fe–N	1	2.11 (1)	0.020 (3)			
Fe⋯C	4	2.973 (4)	0.0083 (5)			
Fe–O-C	8	3.162 (6)	0.0106 (6)			
Fe⋯Fe	1	3.360 (3)	0.0075 (3)			
Solid FeC$_6$_1:3:3						
Fe–O	1	1.896 (3)	0.0073 (3)	–6.6 (2)	0.92 (2)	7.43

Table 2 (continued)

Interaction	N	d	σ^2	E_o [a]	S_o^2	F
Fe–O	4	2.006 (3)	0.0053 (2)			
MS (FeO$_4$)	3 × 4	4.012	0.0063 (9)			
Fe–N	1	2.104 (10)	0.0089 (3)			
Fe⋯C	4	2.939 (4)	0.0071 (4)			
Fe–O-C	8	3.142 (7)	0.0096 (8)			
Fe⋯Fe	1	3.358 (4)	0.0080 (4)			
Solid FeC$_6$_1:3:0						
Fe–O	1	1.890 (3)	0.0020 (3)	–7.3 (2)	0.85 (1)	9.54
Fe–O	4	2.009 (2)	0.0050 (2)			
MS (FeO$_4$)	3 × 4	4.018	0.0072 (9)			
Fe⋯C	4	2.997 (5)	0.0080 (5)			
Fe–O–C	8	3.212 (9)	0.0095 (11)			
Fe⋯Fe	1	3.434 (2)	0.0030 (2)			
Aqueous solution, FeC$_6$_1:1, pH 1.67						
Fe–O	1	1.92 (2)	0.003 (1)	–7.8 (5)	0.87 (3)	27.6
Fe–O/N	5	2.035 (8)	0.008 (2)			
Fe⋯Fe	1	3.35 (2)	0.010 (2)			
Aqueous solution, FeC$_6$_1:3, pH 2.50						
Fe–O	1	1.91 (2)	0.003 (1)	–7.7 (5)	0.84 (3)	24.3
Fe–O/N	5	2.05 (1)	0.009 (2)			
Fe⋯Fe	1	3.35 (2)	0.011 (2)			

[a] 1 eV $= 1.602177 \times 10^{-19}$ J

a mean Fe–O bond distance of 1.79 Å, with the Fe–O–Fe bond angle close to linearity. Compounds with a Fe(OH)$_2$Fe bridge have a mean Fe–O bond distance of ca. 2.00 Å, and a mean Fe⋯Fe distance of ca. 3.1 Å. No compounds with a single hydroxo bridge have been reported. However, a large number of compounds with one hydroxo bridge and one or several carboxylate or sulfate groups bridging two iron sites are fairly common with Fe⋯Fe distances in the range 3.2–3.6 Å depending on kind and number of bridging groups [37]. A comparison of the Fe–O and Fe⋯Fe distances obtained from the EXAFS measurements with the survey briefly summarized above strongly indicates that the solid iron(III) alkyl-*N*-iminodiacetate compounds are hydrolyzed with a single hydroxo bridge with one or two acetate groups bridging two iron sites. It is possible that these alkyl-*N*-iminodiacetates bind to different Fe–OH–Fe units in a network structure. In addition, Fe(III) binds at least one alkyl-*N*-iminodiacetate group in a chelate complex, where the Fe–N bond distances differ depending on the pH condition at precipitation, Table 2. In the sample precipitated under the most acidic conditions, FeC$_6$_1:3:0, the nitrogen seems to be protonated and not bound to iron(III). In the solids precipitated at medium pH, FeC$_{12}$_1:1:1, FeC$_{12}$_1:2:1, FeC$_6$_1:1 and FeC$_6$_1:3:3, the Fe–N bond distance is in the order of 2.35 Å, which is in very good agreement with the Fe–N bond distances in the solids containing the [Fe(EDTA)(H$_2$O)]$^-$ complex in the solid state where the nitrogen is deprotonated [37]. In the solid samples precipitated at the highest pH values, the Fe–N bond distance is significantly shorter, ca. 2.11 Å, Table 2.

The EXAFS data of the iron(III)–*n*-hexyl-*N*-iminodiacetate complexes in aqueous solution have low S/N ratio and limited structural information can be extracted. As for the solid samples, the main peak in the FTs, assigned to Fe–O bond distances, is asymmetric, Fig. 2, indicating that the complex in aqueous solution has one shorter Fe–O bond, and therefore is most likely hydrolyzed. It has not been possible to accurately determine the second scattering shell of carboxylate carbons, while a Fe⋯Fe distance is barely possible to recognize. The structure of the iron(III)–*n*-hexyl-*N*-iminodiacetate complex in aqueous solution is most likely dimeric with a hydroxo and diacetate groups bridging the iron(III) irons, which in addition most likely form a chelate complex with *n*-hexyl-*N*-iminodiacetate.

3.3 The Chromium(III)-alkyl-*N*-iminodiacetic Acid Systems in Water

3.3.1 Acid/Base Titrations of Chromium(III)/Methyl-*N*-iminodiacetate (1:2)

The titration functions of Cr^{3+}/methyl-*N*-iminodiacetic acid are shown in Fig. S3. The forward and back titrations are completely different showing the irreversibility of the system. At pH 4.3–4.6 there is a change to a green tone whereas at 5.1–5.2 the color becomes bright lime. At pH 6.2 the pH rises more rapidly and then slowly decreases again, reflecting the slow kinetics of the system, and the color changes to a grayish blue tone. At pH 8, the kinetic effect diminishes and the titration becomes stable and the color changes to a darker grayish-green tone. When back-titrating the alkaline titrand with 0.10 mol·dm^{-3} perchloric acid there is almost no buffering capacity of the titrand at all; the system acts more or less as a non-protolyte. There is a smeared out shoulder in the region between pH 6–7 including a slight dynamic effect in the reading of pH. Below pH 4 the solution becomes blue/violet and does not change color further.

3.3.2 Acid/Base Titrations of Chromium(III)/methyl-*N*-iminodiacetate (1:3)

The titrand was clear and purple/blue with pH = 2.2 from the start. At pH = 3.5–3.8 the titrand took on a turquoise tone and at pH = 4.1–4.2 the titrand became greenish black and opaque. When one mole equivalent of sodium hydroxide (with respect to chromium) was added, partial precipitation was observed. The precipitate was gluey and obviously different from the common green chromium(III) hydroxide. The dried precipitate was amorphous and glassy.

3.3.3 Solubility of Precipitate from Chromium(III)/Hexyl-*N*-iminodiacetate 1:3 at pH 4.21 in Chloroform

The dried precipitate of chromium(III)/*n*-hexyl-*N*-iminodiacetic acid (1:3) obtained at pH 4.21 after titration with 0.1 mol·dm^{-3} sodium hydroxide to pH 4.21, was added to chloroform and set for gentle shaking for 48 h. The solvent becomes slightly opaque with a bluish tone but the major part of the solid remained undissolved, and no significant change in viscosity was observed. This indicates that the precipitate mainly consists of a polymeric structure.

3.3.4 EXAFS Analysis on Chromium(III)/*n*-Hexyl-*N*-iminodiacetate Complexes in Solution and as a Paste

The Fourier transforms of the studied chromium samples are shown in Fig. S4 (the data are not corrected for the phase shift). The major peak at ca. 2.0 Å observed in both chromium(III) samples corresponds to a first shell of oxygen atoms in an octahedral configuration, and the corresponding multiple scattering within the inner CrO_6 coordination core is observed at ca. 3.9 Å. In the paste sample there is a peak at 2.8 Å corresponding to a second coordination shell of carbons, and the corresponding 3-leg Cr–O–C multiple scattering path is observed at 3.3 Å. The best fit of the chromium EXAFS data is with an octahedral model with d(Cr–O) = 1.96 and 1.98 Å, and d(Cr–O_{MS}) = 3.9 Å, in the solid and the aqueous solution, respectively. In the solid state a second shell of carbon atoms is found for d(Cr···C) = 2.89 Å and a multiple scattering path for d(Cr–O–C) = 3.17 Å is observed as well, corresponding to a Cr–O–C angle of about 125°. The fit to the EXAFS functions was not improved by adding nitrogen or chromium distances as back-scatterers to the model. This indicates that the *n*-hexyl-*N*-iminodiacetate ligands are bridging chromium(III) ions in the solid state in a similar way as described for the solid iron(III) system above. Distances and refined structure parameters are given in Table 3, and the fitted EXAFS data with these parameters are shown in Fig. 4.

3.4 Comparison of Complex Formation Ability of Calcium, Iron(III) and Chromium(III) with Alkyl-*N*-iminodiacetate

Calcium forms very weak complexes with alkyl-*N*-iminodiacetates in aqueous solution, and thus carboxylated polyamines cannot be used for separation of calcium from wastewater. Iron(III) and chromium(III) form both strong complexes with alkyl-*N*-iminodiacetates, which readily precipitate. Iron(III) hydrolyzes easily and all compounds contains a dimeric entity where a hydroxo group and one or two acetate groups bridge iron(III) in alkyl-*N*-iminodiacetate chelate complexes. In these complexes the nitrogen atom is significantly more weakly bound than the oxygens. It seems likely that the low solubility in water is caused by the alkyl-*N*-iminodiacetates bridging the iron sites in one dimer also binding to another dimer through the other acetate group. Chromium(III) seems to only bind oxygen atoms from acetate groups, and that the alkyl-*N*-iminodiacetates bridge

Table 3 Mean bond distances, d/Å, Debye–Waller factors, σ^2/Å^2, number of distances, N, and the shift in the threshold energy, ΔE_o/eV, of chromium(III)–*n*-hexyl-*ss* complexes in solid state at room temperature

Interaction	N	d	σ^2	ΔE_o[a]	S_o^2
Cr^{3+}/*n*-hexyl-*N*-iminodiacetic acid/OH$^-$ (1:3:3)solid					
Cr–O	6	1.974 (2)	0.0041 (2)	− 13.3 (2)	0.73 (2)
Cr···C	3	2.82 (1)	0.005 (3)		
Cr–O–C	6	3.07 (2)	0.006 (2)		
MS(CO$_6$)	3×6	3.94 (1)	0.007 (2)		
Cr^{3+}/*n*-hexyl-*N*-iminodiacetic acid/OH$^-$ (1:3:3)–aqueous solution, 58 mmol·dm^{-3}					
Cr–O	6	1.970 (6)	0.0024 (7)	− 12.7 (6)	0.74 (3)
Cr···C	3	2.83 (2)	0.005 (−)		
Cr–O–C	6	3.06 (2)	0.008 (2)		
MS(CO$_6$)	3×6	3.94 (2)	0.008 (2)		

two chromium(III) ions is in a three-dimensional network explaining the low solubility of these compounds. Iron(III) and chromium(III) both form insoluble compounds with alkyl-*N*-iminodiacetates but the structures are significantly different. Carboxylated polyamines seems to be feasible collectors of these ions for the separation from wastewaters.

4 Conclusions

The calcium(II) ion forms only one weak monodentate complex with methyl-*N*-iminodiacetate in water, $K_1 = 12.9$ (2) $mol^{-1} \cdot dm^3$. The calcium(II) alkyl-*N*-iminodiacetate complexes are octahedral in the solid state with, most probably, water in the remaining positions with a mean Ca-O bond distance of ca. 2.36 Å.

By mixing iron(III), alkyl-*N*-iminodiacetate and sodium hydroxide in different ratios, pale orange compounds precipitate. The structure determination of these solids has been performed by EXAFS as it has not been possible to obtain any crystals with sufficient size and quality for crystallographic studies. The EXAFS studies show that iron(III) is hydrolyzed in all studied compounds, seen in a well-defined Fe····Fe distance of 3.35–3.43 Å. The Fe····Fe distance and a Fe–O bond distance of ca. 1.9 Å, strongly indicating a structural motif with hydroxo group and one or two acetate groups bridging the iron(III) complexes. In addition, iron(III) binds one or two alkyl-*N*-iminodiacetates as a chelate complex. In the compound formed at the lowest pH value, FeC_6_1:3:0, the nitrogen atom seems not to bind to iron(III), and is therefore most likely protonated. In the other compounds iron(III) binds very weakly to nitrogen with an Fe–N bond distance of 2.35 Å, which is in close agreement with the binding to other carboxylated amines such as EDTA [37]. In the compounds precipitated at the highest pH values the Fe–N bond distance is shorter. The structures of the iron(III) alkyl-*N*-iminodiacetate complexes in aqueous solution indicate that they are hydrolyzed in a similar way as in the solids.

Chromium(III) forms fairly strong complexes with alkyl-*N*-iminodiacetates. The complexes are octahedral both in solution and the solid state, and the low solubility of solid compounds indicates a polymeric structure with the ligands bridging between chromium(III) ions. Chromium(III) binding of the oxygen atoms in carboxylated amines/polyamines is significantly stronger and at shorter distance than the nitrogen atoms. The chromium(III) alkyl-*N*-iminodiacetate complexes display such slow kinetics during the titration of strong acid and base that in fact the reactions are completely irreversible.

Hard metal ions with high charge density, such as iron(III) and chromium(III), form insoluble compounds with alkyl-*N*-iminodiacetate ligands making them hydrophobic and thereby possible to separate from aqueous systems. Carboxylated polyamines should therefore an interesting group chelating surfactants for the separation of iron(III) and chromium(III) from wastewaters.

References

1. Porter, M.R.: Handbook of Surfactants, 2nd edn. Blackie Academic & Professional, London (1994)
2. IUPAC Stability Constants Database, Academic Software. Sourby Old Farm, Timble, Otley, Yorks, LS21 2PW (2016); https://www.acadsoft.co.uk
3. Polyakova, I.N., Poznyak, A.L., Sergienko, V.S.: Crystal structures of strontium and calcium acid iminodiacetates Sr(HIda)$_2$·5H$_2$O and Ca(HIda)$_2$. Russ. J. Inorg. Chem. **48**, 1998–2004 (2003)
4. Mukkamala, S.B., Anson, C.E., Powell, A.K.: Modelling calcium carbonate biomineralisation processes. J. Inorg. Biochem. **100**, 1128–1138 (2006)
5. Walters, M.A., Vapnyar, V., Bolour, A., Incarvito, C., Rheingold, A.L.: Iron(III) nitrilotriacetate and iron(III) iminodiacetate, Their X-ray crystallographic structures and chemical properties. Polyhedron **22**, 941–946 (2003)
6. Wang, J., Zhang, W.Q., Song, X.M., Zhang, X.D., Xing, Y., Lin, Y.H., Jia, H.Q., Zhang, L.: Investigation on molecular and crystal structures of metal complexes with aminopolycarboxylic acids: Synthesis and structure of Na$_2$[FeIII(ida)$_2$]$_2$·3H$_2$O. Chin. Chem. Lett. **8**, 741–744 (1997)
7. Schmitt, W., Jordan, P.A., Henderson, R.K., Moore, G.R., Anson, C.E., Powell, A.K.: Synthesis, structures and properties of hydrolytic Al(III) aggregates and Fe(III) analogues formed with iminodiacetate-based chelating ligands. Coord. Chem. Rev. **228**, 115–126 (2002)
8. Meier, R., Molinier, M., Anson, C., Powell, A.K., Kallies, B., van Eldik, R.: Structure of sodium bis(*N*-methyl-iminodiacetato)iron(III): *trans*-meridional *N*-coordination in the solid state and in solution. Dalton Trans **46**, 5506–5514 (2006)
9. Clegg, W., Powell, A.K., Ware, M.J.: Structure of trisodium bis(nitrilotriacetato)ferrate(III) pentahydrate, Na$_3$[Fe{N(CH$_2$CO$_2$)$_3$}$_2$]·5H$_2$O. Acta Crystallogr. Sect. C **40**, 1822–1824 (1984)
10. Mootz, D., Wunderlich, H.: Potassium *cis*-bis(iminodiacetato)chromate(III) trihydrate. Acta Crystallogr. Sect. B **36**, 445–447 (1980)
11. Li, H., Xu, D.-J., Lin, K.-L.: Sodium cis-bis(iminodiacetato-κ3N,O′)chromate(III) sesquihydrate. Acta Crystallogr. Sect. E **59**, m671–m673 (2003)
12. Zabel, M., Pawlowski, V.I., Poznyak, A.L.: Crystal structure of calcium *cis*(N)-bis(iminodiacetato) chromate(III) nonahydrate Ca[Cr(Ida)$_2$]$_2$·9H$_2$O. J. Struct. Chem. **50**, 582–584 (2009)
13. Moon, D., Choi, J.-H.: Crystal structure of ammonium/potassium trans-bis(N-methyliminodiacetato-κ3O, N, O′)chromate(III) from synchrotron data. Acta Crystallogr. Sect. E **72**, 1190–1193 (2016)
14. Suh, J.-S., Park, S.-J., Lee, K.-W., Suh, I.-H., Lee, J.-H., Song, J.-H., Oh, M.-R.: Sodium trans-bis(methyliminodiacetato-O,O)chromate(III), Na[Cr(C$_5$H$_7$NO$_4$)$_2$]. Acta Crystallogr. Sect. C **53**, 432–434 (1997)
15. Suh, I.-H., Lee, J.-H., Song, J.-H., Oh, M.-R., Suh, J.-S., Park, S.-J., Lee, K.-W.: Two possible space Groups *P*1 and *A*2/*n* of sodium *trans*-bis(methyliminodiacetato)chromate(III). J. Korean Phys. Soc. **29**, 739–744 (1996)
16. Mootz, D., Wunderlich, H.: Sodium *trans*-bis(*N*-isopropyliminodiacetato)chromate(III) dihydrate. Acta Crystallogr. Sect. B **36**, 721–722 (1980)
17. Mootz, D., Wunderlich, H.:Potassium *trans*-bis(*tert*-butyliminodiacetato)chromate(III) tetrahydrate. Acta Crystallogr., Sect. B **36**, 1189–1191 (1980)
18. Gabriel, C., Raptopoulou, C.P., Terzis, A., Lalioti, N., Salifoglou, A.: Synthesis, structural, spectroscopic and magnetic susceptibility studies of a soluble Cr(III)–HEIDA (2-hydroxyethyliminodiacetic acid) complex: Relevance to aqueous chromium(III)–HEIDA speciation. Inorg. Chim. Acta **360**, 513–522 (2007)
19. Visser, H.G., Purcell, W., Cloete, N., Muller, A.: Caesium bis[*N*-(carbamoylmethyl)iminodiacetato] chromate(III) dihydrate. Acta Crystallogr. Sect. E **61**, m1668–m1670 (2005)

20. Liu, Y.Y., Zhai, B., Cai, H., Ding, B., Zhao, X.-J.: Synthesis and characterization of silver(I) and het-erometallic Cr(III)–Na compounds with the tripodal ligand *N*-(carbamoylmethyl)iminodiacetic acid. Transition Metal Chem. **34**, 629–635 (2009)

21. Visser, H.G.: Caesium bis[*N*-(carboxymethyl)iminodiacetato]chromate(III) dihydrate. Acta Crystallogr. Sect. E **63**, m162–m164 (2007)

22. Häggman, L., Lindblad, C., Oskarsson, H., Ullström, A.-S., Persson, I.: The influence of short strong hydrogen bonding on the structure and the physicochemical properties of alkyl-*N*-iminodiacetic acids in solid state and aqueous systems. J. Am. Chem. Soc. **125**, 3631–3641 (2003)

23. Jalilehvand, F., Spångberg, D., Lindqvist-Reis, P., Hermansson, K., Persson, I., Sandström, M.: Hydration of the calcium Ion: an EXAFS, large-angle X-ray scattering, and molecular dynamics simulation study. J. Am. Chem. Soc. **123**, 431–441 (2001)

24. Sandell, A.: Physical Chemistry 1, Lund University, Lund Sweden, personal communication; the source code is available from the corresponding author of this paper

25. Thompson, A., Attwood, D., Gullikson, E., Howells, M., Kim, K.-J., Kirz, J., Kortright, J., Lindau, I., Liu, Y., Pianetta, P., Robinson, A., Scofield, J., Underwood, J., Williams, G., Winick, H.: X-ray Data Booklet, 3rd edn., Lawrence Berkley National Laboratory (2009)

26. George, G.N., Pickering, I.J.: EXAFSPAK – a suite of computer programs for EXAFS analysis, SSRL, Stanford University, CA (1993)

27. Zabinsky, S.I., Rehr, J.J., Ankudinov, A.L., Albers, R.C., Eller, M.J.: Multiple-scattering calculations of X-ray absorption spectra. Phys. Rev. B **52**, 2995–3009 (1995); Ankudinov, A. L., Rehr, J. J.:Relativistic calculations of spin-dependent X-ray absorption spectra. Phys. Rev. B **56**, R1712–R1716 (1997); The FEFF program available from https://feff.phys.washington.edu/feff.

28. Schubert, J., Richter, J.W.: The use of ion exchangers of the determination of physical-chemical properties of substances, particularly radiotracers, in solution. I. Theoretical. J. Phys. Chem. **52**, 340–350 (1948)

29. Nancollas, G.: Thermodynamics of ion association. Part II. Alkaline earth acetates and formates. J. Chem. Soc. **147**, 744–749 (1956)

30. Archer, D., Monk, C.: Ion-association constants of some acetates by pH (glass electrode) measurements. J. Chem. Soc. **20**, 3117–3122 (1964)

31. de Robertis, A., Di Giaomo, P., Foti, C.: Ion-selective electrode measurements for the determination of formation constants of alkali and alkaline earth metals with low-molecular weight ligands. Anal. Chim. Acta **300**, 45–51 (1995)

32. Fein, J.: Experimental study of aluminum, calcium, and magnesium acetate complexing at 80 °C. Geochim. Cosmochim Acta **55**, 955–964 (1991)

33. Konigsberger, E., Tran Ho, L.-C.: Solubility of substances related to urolithiasis-experiments and computer modelling. Curr. Tops. Solution Chem. **2**, 183–202 (1997)

34. Streit, J., Tran Ho, L.-C., Konigsberger, E.: Solubility of the three calcium oxalate hydrates in sodium chloride solutions and urine-like liquors. Monatsh. Chem. **129**, 1225–1236 (1998)

35. Armen, G.B., Åberg, T., Karim, K., Levin, J., Crasemann, B., Brown, G., Chen, M., Ice, G.: Threshold double photoexcitation of argon with synchrotron radiation. Phys. Rev. Lett. **54**, 182–185 (1985)

36. Ito, Y., Nakamatsu, H., Mukoyama, T., Omote, K., Yoshikado, S., Takashi, M., Emura, S.: Multielectron transitions in X-ray absorption of krypton. Phys. Rev. A **46**, 6083–6086 (1992)

37. Allen, F.H.: The Cambridge Structural Database: A quarter of a million crystal structures and rising. Acta Crystallogr. Sect. B **58**, 380–388 (2002). **and references cited therein**

Affiliations

Cecilia Lindblad[1] · Anders Cassel[2,3] · Ingmar Persson[1]

1   Department of Molecular Sciences, Swedish University of Agricultural Sciences, P.O. Box 7015, SE-750 07 Uppsala, Sweden

2   Nouryon Surface Chemistry AB, Stenunge allé 3, SE-44430 Stenungsund, Sweden

3   Present Address: SE-471 60 Myggenäs, Sweden